An in silico structural approach to characterize human and rainbow trout estrogenicity of mycotoxins

Luca Dellafiora, Isabelle P. Oswald, Jean-Lou Dorne, Gianni Galaverna, Paola Battilani, Chiara Dall'Asta

An *in silico* structural approach to characterize human and rainbow trout estrogenicity of mycotoxins: Proof of concept study using zearalenone and alternariol

Luca Dellafiora[1*], Isabelle P. Oswald[2], Jean-Lou Dorne[3], Gianni Galaverna[1], Paola Battilani[4], Chiara Dall'Asta[1]

[1] Department of Food and Drug, University of Parma, Area Parco delle Scienze 27/A, 43124 Parma, Italy
[2] Toxalim (Research Centre in Food Toxicology), Université de Toulouse, INRA, ENVT, INP-Purpan, UPS, 31027 Toulouse, France
[3] European Food Safety Authority (EFSA),
[4] Department of sustainable crop production, Università Cattolica del Sacro Cuore, Via Emilia Parmense 84, 29122 Piacenza, Italy

* Correspondence to:
Luca Dellafiora. Department of Food and Drug, University of Parma, Area Parco delle Scienze 27/A, 43124 Parma, Italy. Phone: +390521906196. Email: luca.dellafiora@unipr.it

Authors email: Luca Dellafiora, luca.dellafiora@unipr.it; Isabelle P. Oswald, isabelle.oswald@inra.fr; Jean-Lou Dorne, Jean-Lou.DORNE@efsa.europa.eu; Gianni Galaverna, gianni.galaverna@unipr.it; Paola Battilani, paola.battilani@unicatt.it; Chiara Dall'Asta, chiara.dallasta@unipr.it

Abstract

The mycotoxins zearalenone and alternariol may contaminate food and feed raising toxicological concerns due to their estrogenicity. Inter-species differences in their toxicokinetics and toxicodynamics may occur depending on evolution of taxa-specific traits. As a proof of principle, this manuscript investigates the comparative toxicodynamics of zearalenone, its metabolites (alpha-zearalenol and beta-zearalenol), and alternariol with regards to estrogenicity in humans and rainbow trout. An *in silico* structural approach based on docking simulation, pharmacophore modeling and molecular dynamics was applied and computational results were analyzed in comparison with available experimental data. The differences of estrogenicity among species of zearalenone and its metabolites have been structurally explained. Also, the low estrogenicity of alternariol in trout has been characterized here for the first time. This approach can provide a powerful tool for the characterization of interspecies differences in mycotoxin toxicity for a range of protein targets and relevant compounds for the food-and feed-safety area.

Keywords: mycotoxins, zearalenone, alternariol, estrogen receptors, in silico toxicology, toxicodynamic

1. Introduction

Zearalenone (ZEN) belongs to a group of mycotoxins of public and animal health concern due to its distribution worldwide, the frequencies and the levels of contamination in food and feed, and the severity of adverse effects it may evoke in living organisms (Dong, Pan, Wang, Ahmed, Liu, Peng, et al., 2018). From a chemical point of view, ZEN is a low-molecular weight secondary metabolite produced by fungi belonging to *Fusarium spp*., mainly *F. culmorum* and *F. graminearum* (Marin, Ramos, Cano-Sancho, & Sanchis, 2013). It is chemically described as 6-(10-hydroxy-6-oxo-trans-1-undecenyl)-beta-resorcylic acid lactone (Figure 1). ZEN, along with a number of cognate metabolites, can be found as contaminant in small grains, maize and derived products. The reduced metabolites α-zearalenol and β-zearalenol (αZEL and βZEL, respectively) are among the most abundant forms co-occurring with ZEN (Gromadzka, Waskiewicz, Chelkowski, & Golinski, 2008), though they may be produced significantly also by the phase I metabolism of mammals (EFSA, 2011). Besides evidences pointing to cytotoxic and genotoxic effects, ZEN and its metabolites pose a health risk for humans and animals mainly on account of their xenoestrogenic activity (EFSA, 2011). The main molecular mechanism underlying estrogenicity of ZEN and its metabolites requires the direct binding and activation of estrogen receptors (ERs), which are ligand-induced intracellular transcriptional factors belonging to the nuclear receptor superfamily (Brzozowski, Pike, Dauter, Hubbard, Bonn, Engström, et al., 1997; Spyrakis & Cozzini, 2009).

Several research efforts have described marked interspecies differences in terms of susceptibility to the stimulation by ZEN and its metabolites (EFSA, 2017). In this respect, pigs are amongst the most sensitive species (Binder, Schwartz-Zimmermann, Varga, Bichl, Michlmayr, Adam, et al., 2017), while chicken are more resistant (Pitt, 2013). Inter-species differences in the toxicokinetic profiles of ZEN and its metabolites in animal species have been recognized as the rationale behind species susceptibility and sensitivity (EFSA, 2017; Mally, Solfrizzo, & Degen, 2016; Zinedine, Soriano, Moltó, & Mañes, 2007). Specifically, sensitive species primarily produce metabolites with larger estrogenic potency compared with ZEN and this has been demonstrated for the phase-I metabolite αZEL (Binder, et al., 2017). Conversely, species that are more resistant to the toxicity of ZEN tend to produce larger amount of metabolites with estrogenic potency lower than that from ZEN such as the phase I metabolite βZEL (Devreese, Antonissen, Broekaert, De Baere, Vanhaecke, De Backer, et al., 2015). However, interspecies differences in toxicokinetics (TK) may not fully account for species susceptibility and sensitivity to ZEN and toxicodynamic (TD) differences may also play a role in sensitivity among species, though they are not commonly considered. In this regard, inter-species differences in the primary sequences of estrogen receptors (ERs) may impact binding of ZEN and its metabolites, with subsequent consequences on ERs activation and estrogenic potency (Matthews, Celius, Halgren, & Zacharewski, 2000). In the context of risk assessment, the molecular characterization of such TD differences may provide precious information to better understand the species-specific mechanisms of toxicity and to provide a more through explanation of inter-species differences.

This manuscript deals with the comparative modelling of the estrogenic activity of ZEN, αZEL and βZEL in human and rainbow trout (*Oncorhynchus mykiss*) to investigate interspecies differences as a proof of principle. To do so, a computational workflow based on molecular modelling techniques has been used. Notably, computational methods provides valuable tools for the characterization of biological and toxicological properties of a wide spectrum of molecules (e.g. (Cheron, Casciuc, Golebiowski, Antonczak, & Fiorucci, 2017; L. Dellafiora, Dall'Asta, Cruciani, Galaverna, & Cozzini, 2015; Ivanova, Karelson, & Dobchev, 2018; Lin, Zhang, Han,

Xin, Meng, Gong, et al., 2018)).
In addition, the estrogenic potential of alternariol (AOH), an emerging mycotoxin with estrogenic properties produced by *Alternaria spp.* (L. Dellafiora, Warth, Schmidt, Del Favero, Mikula, Fröhlich, et al., 2018), has also been assessed. Deepening the understanding of the molecular aspects of ZEN and AOH estrogenicity in trout is also very relevant given the overall paucity of data and the poor understanding of mycotoxins action in fish, even though a number of mycotoxins, including ZEN and AOH, constitute emerging hazards to fish health in rivers and modern aquaculture (Gonçalves, Schatzmayr, Albalat, & Mackenzie, 2018; Tolosa, Font, Manes, & Ferrer, 2014).
In this context, the computational study presented here applies a workflow based on pharmacophoric modelling, docking simulation and molecular dynamics, which has already demonstrated to reliably model bioactivity and toxicity of low-molecular weight compounds (e.g. ref. (L. Dellafiora, Dall'Asta, Cruciani, Galaverna, & Cozzini, 2015)). Specifically, this work aims to: i) Model at the molecular level the diverse inter-species toxicodynamics of ZEN, αZEL and βZEL with regards to their interaction with ERs using a structural approach. In this respect, the computational modeling may be a rapid and cost-effective analytical method to valuably integrate data from *in vitro* and *in vivo* trials in the risk assessment process (L. Dellafiora, Dall'Asta, & Galaverna, 2018; Lewis, Kazantzis, Fishtik, & Wilcox, 2007). ii) Characterize inter-species differences in ERs binding to provide a mechanistic understanding of ZEN-related effects among species. iii) Extend knowledge of the interspecies differences in AOH toxicity, which is considered among the emerging mycotoxins of most concern (Gruber-Dorninger, Novak, Nagl, & Berthiller, 2017).

2. Materials and methods

2.1. Design of the human and rainbow trout estrogen receptor models

The model of the alpha isoform of human ER (hERa) ligand binding domain was designed from the ZEN-bound crystallographic structure deposited in the RCSB PDB databank (http://www.rcsb.org) with ID code 5KRC (chain A) (Nwachukwu, Srinivasan, Bruno, Nowak, Wright, Minutolo, et al., 2017). The structure was processed using the Sybyl software, version 8.1 (www.certara.com) checking the consistency of atom and bond types assignment and removing the co-crystalised ligand and waters, as previously reported (L. Dellafiora, Galaverna, Dall'Asta, & Cozzini, 2015). The protein presented unresolved coordinates in the regions 332-335 and 461-472. The sequence continuity in the region 461-472 was achieved using the "Align Structure by Homology" tool of the Biopolymer module of Sybyl software, version 8.1 (www.certara.com) by superimposing the human ERα structure with PDB code 2YJA (Phillips, Roberts, Schade, Bazin, Bent, Davies, et al., 2011) and linking to the model the corresponding atomic coordinates of such region. Conversely, the continuity of the region 332-335 was achieved using the Loop/Refine module of Modeler software (version 9.1) (Sali & Blundell, 1993) interfaced in the UCSF Chimera software (version 1.11) (Pettersen, Goddard, Huang, Couch, Greenblatt, Meng, et al., 2004) limiting the structure refinements at the missing part only. The number of models to generate was set at five and only the best scored model according to GA341 and zDOPE scores was considered.
Since no rainbow trout ER (rtER) structures were available in the PDB databank (http://www.rcsb.org) (last database access in January 17th, 2019), the 3D model of the rainbow trout ERα ligand binding domain (NCBI Reference Sequence: NP_001117821.1; residues 323-560) was achieved through homology modeling using the hER model as a template, as

previously reported (L. Dellafiora, Dall'Asta, & Cozzini, 2015) within the software Modeler (version 9.1) (Sali & Blundell, 1993) interfaced in the UCSF Chimera software (version 1.11) (Pettersen, et al., 2004) . The root-mean square deviation (RMSD) analysis of proteins backbone between trout model and its human template was done using the "Compare Structures" tool of the Biopolymer module of Sybyl software, version 8.1 (www.certara.com).
For sequence analysis, the global pairwise alignment of ER ligand binding domains primary sequence was conducted using the on-line tool EMBOSS-Water Pairwise Sequence Alignment (http://www.ebi.ac.uk) and the Needleman-Wunsch alignment algorithm.

2.2 Pharmacophoric modelling

The binding site of both hERα and rtERα models was defined using the Flapsite tool of the FLAP software together with the GRID algorithm to investigate the corresponding pharmacophoric space (Baroni, Cruciani, Sciabola, Perruccio, & Mason, 2007; Carosati, Sciabola, & Cruciani, 2004). The DRY probe was applied to describe potential hydrophobic interactions, while the sp2 carbonyl oxygen (O) and the neutral flat amino (N1) probes were used to describe the hydrogen bond acceptor and donor capacity of the target, respectively.

2.3 Docking simulations

GOLD (Genetic Optimization for Ligand Docking) software was chosen to perform docking studies as the appropriate tool for computing protein-ligand interactions (e.g. (Maldonado-Rojas & Olivero-Verbel, 2011; Rollinger, Schuster, Baier, Ellmerer, Langer, & Stuppner, 2006)). The occupancy of the binding site was set within a sphere 10 Å around the centroid of the pocket. Software setting and docking protocol previously reported were used (L. Dellafiora, Galaverna, & Dall'Asta, 2017). As an exception, the use of external scoring functions was omitted as the GOLD's internal scoring function GOLDScore succeeded in analyzing the reference set of compounds (*vide infra*). Specifically, GOLDScore fitness considers the external (protein-ligand complex) and internal (ligand only) van der Waals energy, protein-ligand hydrogen bond energy and ligand torsional strain energy. In each docking study, the proteins were kept semi-flexible and the polar hydrogen atoms were set free to rotate. The ligands were set fully flexible.
GOLD implements a genetic algorithm that may introduce variability in the results. Therefore, testing of the models were performed in triplicates and results were expressed as mean ± standard deviation (SD) ratio to the reference compound E2 to ensure causative scores assignments for ER binding. In addition, molecules showing multiple poses and/or low and variable score (coefficient of variation > 10%) were considered a priori unable to favorably bind the pocket being unable to find a stable binding pose and were not included in the statistical analysis (L Dellafiora, Galaverna, Cruciani, Dall'Asta, & Bruni, 2018). .

2.4 Molecular dynamic

Molecular dynamic (MD) simulations were performed to investigate the dynamic of ligands interaction with the ligand binding site of both human and trout ER, in comparison to those of the endogenous agonist E2. The best scored binding poses calculated by docking simulation were used as input for MD. MD simulations were performed using GROMACS (version 5.1.4) (Abraham, Murtola, Schulz, Páll, Smith, Hess, et al., 2015) with CHARMM27 all-atom force field parameters support (Best, Zhu, Shim, Lopes, Mittal, Feig, et al., 2012). All the ligands have been processed and parameterized with CHARMM27 all-atom force field using the SwissParam tool (http://www.swissparam.ch). Crystallographic waters kept in the docking studies were

removed and protein-ligand complexes were solvated with SPCE waters in a cubic periodic boundary condition, and counter ions (Na^+ and Cl^-) were added to neutralize the system. Prior to MD simulation, the systems were energetically minimized to avoid steric clashes and to correct improper geometries using the steepest descent algorithm with a maximum of 5,000 steps. Afterwards, all the systems underwent isothermal (300 K, coupling time 2psec) and isobaric (1 bar, coupling time 2 psec) 100 psec simulations before running 50 nsec simulations (300 K with a coupling time of 0.1 psec and 1 bar with a coupling time of 2.0 psec).

2.5 Statistical analysis

Statistical analysis of docking results was performed using IBM SPSS Statistics for Linux, version 25 (IBM Corp., Armonk, NY). The data was analysed by one-way ANOVA ($\alpha = 0.05$), followed by post hoc Fisher's LSD test ($\alpha = 0.05$), except for the paired ratio comparisons that were analyzed using paired student's t test.

3. Results and Discussion

3.1 Design of trout ER model

There are no 3D structures of rainbow trout ER available in the PDB databank (http://www.rcsb.org) (last database access in January 17th, 2019). Therefore, the rainbow trout ER (rbER) model was designed using homology modelling, a technique which can provide reliable 3D models of biological targets when the structure of homologous proteins are available (Lohning, Levonis, Williams-Noonan, & Schweiker, 2017; Monzon, Zea, Marino-Buslje, & Parisi, 2017). Notably, homology modelling may be particularly suitable to model the ligand binding domain of ERs given the strong conservation of 3D structures along the evolutionary path of nuclear receptors, and especially among the ER orthologous (Pike, Brzozowski, & Hubbard, 2000).

The alpha isoform of hER (hERa) was used as a template to model the alpha 1 isoform of rbER. The hERa and rtER orthologous addressed in this study (GenBank accession code AAD52984.1, residues 310-547; and NCBI reference sequence NP_001117821.1, residues 323-560, respectively) shared 64 % of sequence identity and 81 % of sequence similarity (according to BLOSUM62 matrix) respectively. To note, sequences sharing an identity higher than 50% are typically though to provide high-confidence models (Dalton & Jackson, 2007). In addition, the root-mean squared deviation (RMSD) analysis of proteins backbone between the model and its template was done to further check the model confidence. The very low value recorded (0.74 Å) pointed to the high confidence of the model used, in agreement with previous studies (Nikolaev, Shtyrov, Panov, Jamal, Chakchir, Kochemirovsky, et al., 2018). With regards to the ligand binding pockets, the sequence appeared highly conserved with the exception of L349/362M and M528/541I substitutions (according to human and fish numeration, respectively) (Figure 2). The geometrical reliability of rbER was checked comparing the model with the crystallographic structures of hER. As shown in Figure 2, the overall geometrical organization of rbER was correctly predicted in terms of ternary structure and in terms of arrangement of pocket architecture and spatial distribution of residues, thereby supporting its use as reliable model for the following analysis.

3.2 Pharmacophoric modeling

The pharmacophoric fingerprint of the human and trout ERs ligand binding domain pocket has been computed using the FLAP software (further details are reported in Section 2.2). The fingerprints of the two ER orthologous in terms of distribution of hydrophobic and hydrophilic

space appeared mainly hydrophobic with two polar patches at the two pocket terminus formed by Glu353/366, Arg394/407 and His524/537, as previously described (L. Dellafiora, Galaverna, Dall'Asta, & Cozzini, 2015). Nevertheless, the M528/541I mutation was observed causing a slight pocket reshape that resulted into an extension of the hydrophobic space in hER in comparison to rbER (Figure 2).

3.3 Docking simulations

Docking simulations may reliably assess the bioactivity/toxicity of small molecules, as demonstrated previously (Maldonado-Rojas & Olivero-Verbel, 2011; Rollinger, Schuster, Baier, Ellmerer, Langer, & Stuppner, 2006). In particular, molecular modeling approaches able to estimate the capability of ligands to dock the ligand pocket of the ERs agonist conformation may succeed in assessing their (xeno)estrogenic activity (L. Dellafiora, Galaverna, Dall'Asta, & Cozzini, 2015; Ehrlich, Dellafiora, Mollergues, Dall'Asta, Serrant, Marin-Kuan, et al., 2015). However, a fit-for-purpose feasibility assessment of both models was performed comparing the experimental data of ZEN, αZEL and βZEL estrogenicity with the scores respectively calculated. The endogenous ligand E2 and the estrogenically inactive β-sitosterol were taken as positive and negative controls, respectively. In addition, the calculated poses of E2, ZEN and αZEL were compared to the crystallographic architectures available so far to assess the geometrical reliability of models.

As reported in Table 1, the docking procedure reliably categorized the set of compounds in both models, reflecting the capability to properly compute the different capability of molecules to comply with the physico-chemical properties of the two ER pockets. In particular, the estrogenically inactive β-sitosterol recorded negative scores in both models pointing to its unsuitability to satisfy the physico-chemical requirements of pockets. In addition, the high variability of scores (coefficient of variations ≥ 15%) suggested its incapability to stably arrange into the ligand pocket. On this basis, it was deemed unable to dock the pocket of the agonist conformation of ER and it was computed unlikely to act as ER agonist, in agreement with experimental data (Matthews, Celius, Halgren, & Zacharewski, 2000). Conversely, E2, αZEL, ZEN and βZEL recorded in both models high and positive scores that were significantly different from each other ($p < 0.001$ according to Fisher'LSD post hoc) and properly ranked according to experimental data.

It is worth noticing that the mycotoxins under analysis had a diverse sensitivity in the two species under analysis (Table 1): while αZEL showed an estrogenic potency comparably higher than ZEN in the two species (4-fold and 5-fold higher than ZEN in human and trout, respectively), βZEL appeared much less potent in trout than in human (about 800-fold and 2-fold weaker than ZEN in trout and human, respectively). From a semi-quantitative point of view, the computational analysis reliably computed such differences, being the computed ZEN/βZEL scores ratio significantly higher in trout than in human (i.e. 1.84 ± 0.01 and 1.28 ± 0.02, respectively; $p < 0.001$). Conversely, the computed ZEN/αZEL scores ratios were not statistically different between the two species (i.e. 0.96 ± 0.01 and 0.97 ± 0.00 in human and trout, respectively; $p = 0.37$), pointing to a comparable relative activity in both systems, in agreement with data reported in the literature (Le Guevel & Pakdel, 2001). Therefore, the relative potency of αZEL and βZEL to ZEN could be reliably estimated in both species on the basis of the scores respectively computed. Conversely, the relative potencies of ZEN and αZEL to E2 couldn't be modeled quantitatively in neither of the two species, even though the overall potency rank of compounds was correctly predicted in both models. Indeed, according to

experimental data, the relative potency of ZEN or αZEL to E2 was found higher in trout than in human (namely, the estrogenicity of ZEN and αZEL in comparison to E2 was found higher in trout than in human) (Table 1). Therefore, the computed scores ratios of ZEN and αZEL to E2 were expected to be higher in trout than in human, but it was recorded the opposite. This outcome pointed to the incapability of models presented to correctly predict the quantitative relative potency among different classes of compounds. This finding was in agreement with previous data highlighting that this kind of approaches can be used in quantitative way whether compounds share a strong structural correlation (L. Dellafiora, Dall'Asta, & Cozzini, 2015; Ehrlich, et al., 2015). Conversely, in the case of structurally unrelated compounds, such as ZEN group members and E2, computational scoring can provide a sound rank of potency but are likely to fail in providing (semi)quantitatively reliable relative potency factors. With regards to geometric reliability, the computed poses of E2, ZEN and αZEL were found in strong agreement with the architectures of binding reported by crystallographic studies in terms of pocket occupancy and ligand orientation. This finding finally pointed to the geometrical reliability of both human and trout models (Figure 3). On the basis of these results, both models appeared reliable in predicting the potency rank and the binding geometry of compounds under analysis, even though the relative potency factors could be modeled only within ZEN group.

Then, the binding poses of ZEN, αZEL and βZEL in the two models were inspected to investigate the mechanistic basis of their respective activity and, in particular, to explain the differences in terms of susceptibility to βZEL stimulation between the two species. From the human ER model, differences between ZEN, αZEL and βZEL, which all involved the same binding pose resembling E2 (Figure 3), could be explained in terms of pocket fitting as discussed elsewhere by Ehrlich and co-workers (Ehrlich, et al., 2015). For αZEL, the presence of one hydroxyl group with α isomerism in correspondence to the His524, instead of a ketone as for ZEN, demonstrated to be a preferable feature to stably interact with the pocket, as previously observed for steroid ligands (Sonneveld, Riteco, Jansen, Pieterse, Brouwer, Schoonen, et al., 2006). Structurally, this finding was rationalized through the comparison of the binding poses of αZEL and E2, wherein the α-hydroxyl group of αZEL superimposed the 18-β hydroxyl group of E2 (Figure 3D). Conversely, the hydroxyl group with β isomerism of βZEL likely superimposes the α-hydroxyl group of 17α-estradiol, which is known to cause a reduction of pocket fitting as testified by the lower estrogenicity of 17α-estradiol in comparison to E2 (Sonneveld, et al., 2006).

From the trout ER model, ZEN and αZEL showed the same binding pose recorded in the human model, in spite of the presence of two mutations occurring at the binding site (L349/362M and M528/541I according to human and fish numeration, respectively). A different orientation was found for βZEL instead, as shown in Figure 3E. The slight pocket reshaping due to L349/362M and M528/541I mutations induced βZEL to adopt a pose rotated about 180° onto the longitudinal axis of pseudo-symmetry. In this atypical orientation, the aromatic ring of βZEL was prevented from superimposing the aromatic ring of ZEN, αZEL and E2. Given the strict orientation the aromatic rings must adopt into the pocket, as reported by the huge number of crystallographic data available so far, such an uncommon arrangement did not point to a plausibly relevant capability of βZEL to interact with the pocket. On this basis, the atypical ligand arrangement and uncommon pocket occupancy might explain at least in part the lower capability of βZEL to trigger estrogenic stimuli in trout ER in comparison to the human orthologous.

With regards to AOH, in the human ER model the procedure correctly predicted the potency rank as AOH which was scored below ZEN, in agreement with the lower estrogenic activity

reported in literature (Lehmann, Wagner, & Metzler, 2006). This data further confirmed the procedure reliability in estimating the potency rank of compounds. Notably, to the best of our knowledge, no data were available for the estrogenicity of AOH in trout and, as shown in Table 1, AOH was expected to be qualitatively less potent than ZEN with a lower calculated score. In addition, the comparison between the calculated poses of AOH within the human and trout ER revealed differences in the pocket occupancy (Figure 3F). Indeed, AOH adopted, within the human ER model, an orientation similar to those shown by E2, ZEN and αZEL, which has been largely described by crystallographic studies as the one properly fitting ER pocket. Conversely, AOH within the trout ER model showed an uncommon and distorted orientation that might suggest its unsuitability to properly fit the ER pocket. On this basis, the interaction with the trout ER model can be concluded less likely with a potentially low capability for estrogenic activities in comparison to the interaction with the human ER.

3.4 Molecular dynamics

MD studies were performed to integrate the results of docking simulation with the analysis of molecular movements of ERs upon ligands binding. MDs were performed for ER of both species in complex with E2, taken as positive control, and ZEN and βZEL in the attempt to understand the molecular basis of inter-species differences to βZEL stimulation. It was calculated also the ER-AOH complex to gain structural insights on the mechanisms underlying the estrogenicity of AOH in hER and to predict its potential effects on rbER (to the best of our knowledge no data are available so far with regards to the estrogenic activity of AOH in trout). The trajectory of ligands and the RMSD of protein C-alpha and ligands' atomic coordinates were analyzed to measure the overall structural stability of complexes, which is crucial for determining the estrogenic activity of ligands (*vide infra*).

With regards to hER, as shown in Figure 4A, the complex with E2 was found the more stable with fluctuations of slight intensity that pointed to the overall stability of hER-E2 complex. Conversely, the complex with ZEN showed stable fluctuations resembling the ones of hER-E2 complex up to about 40 nsec of simulation while increasing the geometrical instability hereafter. The RMSD of hER in complex with AOH or βZEL started increasing much earlier than hER in complex with ZEN. This finding might suggest that AOH and βZEL are less suitable than ZEN to stabilize the agonistic conformation of hER, providing a mechanistic explanation to the lower estrogenic potency found experimentally (Le Guevel & Pakdel, 2001; Lehmann, Wagner, & Metzler, 2006). With regards to ligands within hER complexes, the RMSD fluctuations were found stable and almost comparable to each other (Figure 4B). In addition, the number of hydrogen bonds seemed not relevant to discriminate the potency of ligands, though E2 showed the highest number of long-lasting number of hydrogen bonds along the timeframe considered (Figure 4C). On this basis, the overall stability of hER complex could be considered an important parameter to explain the diverse estrogenicity of ligands under investigation being found related to their potency: the more lasting the overall geometrical stability of hER, the more higher the estrogenic potency of ligands. Keeping in mind that the model was derived from the crystallographic structure of hER in the agonist conformation, this finding is in agreement with the current understanding of hER biochemistry which describes the need to keep stable the agonist conformation of ER to elicit ligand-dependent estrogenic stimuli (Ehrlich, et al., 2015; Spyrakis & Cozzini, 2009).

With regards to the rbER, as shown in Figure 5, rbER in complex with E2, ZEN or βZEL was found overall stable and with comparable RMSD fluctuations. Conversely, the complex with

AOH was found more unstable showing an early (from 10 nsec) and marked RMSD increase. As shown for hER, also in the case of rbER the number and lasting of hydrogen bonds was found not directly correlated to the potency of ligands (Figure 5C). For the geometrical stability of ligands, the RMSD fluctuations of ZEN, βZEL and AOH were found more pronounced than the ones of E2. In particular, βZEL showed a drastic and discrete increase of RMSD in the second part of the simulation. The close inspection of the binding poses revealed that such discrete increase was due to a change in ligand orientation, as shown in Figure 5D. Notably, the alternative conformation of βZEL was supposed not complying with the structural requirements of being a good ER ligand mainly due to the improper orientation of the aromatic ring that did not retrace the common arrangement shown by crystallographic studies (Figure 5D). This uncommon pocket occupancy might explain, at least in part, the lower activity of βZEL in rbER in comparison to its activity reported in hER (Le Guevel & Pakdel, 2001). Given the comparable trend of RMSD fluctuations of rbER in complex with the various ligands, the C-alpha root-mean-square fluctuation (RMSF) analysis was performed to check possible local differences in the protein flexibility among the different rbER complexes studied. For the rbER-βZEL complex and using E2 as a reference, an increased local mobility of two key regions related to ER activation was found among the regions showing differential mobility (Figure 5A). In particular, one region included the residues 425-430, which belong to the so defined H8. That region is proximal to the binding pocket and it was found previously related to the dissociation pathway of ER ligands due to an enhanced local disordering (Sonoda, Martinez, Webb, Skaf, & Polikarpov, 2008). Therefore, the results collected in this work pointed to the weakness of βZEL estrogenicity with regards to its incapability to stabilize a long-lasting agonist-like organization ER receptor and a dissociation pathway taking advantage of the increased disorder of H8 can be hypothesized. The second region included the residues 549-557, which forms the so defined H12. Notably, the proper ligand-dependent stabilization of H12 in the agonist conformation is crucial for eliciting estrogenic activity (Brzozowski, et al., 1997; Spyrakis & Cozzini, 2009). Therefore, a ligand-dependent disrupting action on the agonist-like stabilization of H12 likely relates with non-agonistic activity, as shown for ER (partial) antagonists (Brzozowski, et al., 1997; Spyrakis & Cozzini, 2009). On the basis of the results presented above, the markedly low activity of βZEL in rbER could be explained by multiple concerted molecular events. Among them, it could be identified the improper pocket occupancy and the ligand-dependent enhancement of local protein mobility that may facilitate βZEL dissociation and/or impair the proper agonist conformation of ER.

With regards to the ZEN-rbER complex, an increased disorder in comparison to E2 was observed in the region 425-430, similarly to βZEL. Also in this case, the dissociation pathway of ZEN might take advantage of the increased mobility of such region. On the one hand, this finding plausibly explained the lower activity of ZEN in comparison to E2 pointing to a less lasting and more unstable interaction of ZEN with the pocket in comparison to the endogenous ligand E2. On the other hand, the increased mobility of such region, but not in the region of H12, as observed for βZEL, provided a likely explanation to the different estrogenic activity the two mycotoxins showed in rbER.

As a general remark, it is worth noticing the diverse effects that the set of ligands under analysis exerted on the geometrical stability of ER orthologous. In the case of hER, ligands with different potency exerted a clear and graded effect in the overall protein organization, providing a likely rational to understand mechanistically the diverse action they may have: the more they perturb the stabilization of agonist conformation, the weaker their estrogenic potency is, in agreement

with the current understanding of ERs biochemistry (*vide infra*). Conversely, the overall structure of the trout ER protein was found geometrically less affected by ligands than the human orthologous (with the exception of AOH, which caused early disrupting effects on the overall rbER structure; Figure 5). Indeed, in the case of rbER, ligands were found exerting subtle conformational changes at a local level in key regions involved in protein activity rather than disrupting the overall protein organization as observed for hER. This finding is in agreement with the evolutionary biology of ER family and, more in general, with the nuclear receptor super-family. Evolution has pushed nuclear receptors in the direction of being more ligand-specific and more susceptible to ligand modulation (Bridgham, Eick, Larroux, Deshpande, Harms, Gauthier, et al., 2010; Escriva, Delaunay, & Laudet, 2000). Keeping in mind that ERs need to keep stable the agonist conformation to elicit estrogenic response (see above), the fine ligand-dependent tuning inherently depends on the overall plasticity of receptors. Therefore, proteins prone to relevant ligand-induced disorders as the consequence of slight changes on ligands structure (as in the case of ZEN and its metabolites) are reasonably more selective than those with an inherently more stable conformation. On the basis of the few data available so far, rbER and hER, which underwent different evolutionary processes, showed an apparently different ligand selectivity, with rbER showing a lower selectivity being able to bind ligands encompassing a broader chemical space than hER (Matthews, Celius, Halgren, & Zacharewski, 2000). Therefore, the lower dependence of rbER from ligands in terms of overall geometrical stability found in this study provided a reasonable explanation to the apparent diverse ligands selectivity showed by the two ER orthologous in the few experimental trials available so far.
With regards to AOH, the rtER-AOH complex showed an early increase in RMSD values pointing to the overall geometrical instability of the complex. In addition, the RMSF analysis highlighted an increased mobility of the regions forming H8 and H12, as shown for βZEL, and an additional increased mobility in the region 385-397, which is part of the so defined H5. This region surrounds the H12 and concurs, along with H12, to form the so defined AF2 surface groove that mediate the recruitment of co-regulators protein underlying the full activation of ER (Brzozowski, et al., 1997; Phillips, et al., 2011). Disorders in such regions relate to non-agonist folding of ER (Spyrakis and Cozzini, 2009). Therefore, the concerted increases of structural disorder in those regions led to hypothesize the strong agonistic behavior of AOH not likely. On the basis of these results, a weak activity on the rbER accounted in this study could be hypothesized for AOH. Nevertheless, further data need to be collected in the future on the possible effects mediated by the other ER isoforms in order to precisely characterize the estrogenic potency of AOH in trout.

4. Conclusion

The study presented here addressed an inter-species comparative analysis of toxicodynamic aspects of mycotoxins, taking the estrogenicity of ZEN, αZEL, βZEL and AOH in human and trout as a proof of principle. The study illustrated the reliability of using *in silico* structural approaches to assess and understand the inter-species differences of mycotoxins toxicity from a toxicodynamic perspective. Contextually, the study described the structural rationale behind the mechanisms of action underlying the estrogenic activity of ZEN, αZEL, βZEL and AOH in human and trout. Aside the different capability of these mycotoxins to bind and fit the two ER pockets, the possible existence of species-specific structural changes of ER after mycotoxins binding has been investigated. In particular, hER and rtER were found mainly affected by ligand-dependent changes at a global and local level, respectively. With regards to βZEL, a marked

difference in its docking capacity has been shown for the two ER orthologous. Specifically, the architecture of binding calculated in the rtER did not match with the known binding mode characterized in crystallographic studies. Therefore, the diverse capability to fit the ER pocket, along with the differential disrupting effects on the agonist conformation of ER, provided a structural explanation to the diverse potencies βZEL may have on human and trout ER.
On the other hand, AOH, on the basis of all data collected, was considered unable to exert a significant activity on the trout ER. Nevertheless, the thorough evaluation of possible activity on the other ER isoforms, along with the assessment of any relevant AOH metabolite(s), should be assessed critically in the future to provide a thorough molecular characterization of AOH action on trout ER.

Acknowledgments
The work was carried out as part of the MYCHIF EFSA project (GP/EFSA/AFSCO/2016/01). The view expressed in this article are the authors only and do not necessarily represent the views of the European Food Safety Authority. The authors acknowledge the CINECA award under the ISCRA initiative, for the availability of high performance computing resources and support, and Prof. Gabriele Cruciani for the courtesy of FLAP Software (www.moldiscovery.com).

Conflict of interest The authors declare no conflict of interest.

Reference

Abraham, M. J., Murtola, T., Schulz, R., Páll, S., Smith, J. C., Hess, B., & Lindahl, E. (2015). GROMACS: High performance molecular simulations through multi-level parallelism from laptops to supercomputers *SoftwareX, 1-2*, 19-25.

Baroni, M., Cruciani, G., Sciabola, S., Perruccio, F., & Mason, J. S. (2007). A common reference framework for analyzing/comparing proteins and ligands. Fingerprints for Ligands and Proteins (FLAP): theory and application. *Journal of Chemical Information and Modeling, 47*(2), 279-294.

Best, R. B., Zhu, X., Shim, J., Lopes, P. E., Mittal, J., Feig, M., & Mackerell, A. D. J. (2012). Optimization of the additive CHARMM all-atom protein force field targeting improved sampling of the backbone φ, ψ and side-chain χ(1) and χ(2) dihedral angles. *Journal of Chemical Theory and Computation, 8*(9), 3257-3273.

Binder, S. B., Schwartz-Zimmermann, H. E., Varga, E., Bichl, G., Michlmayr, H., Adam, G., & Berthiller, F. (2017). Metabolism of Zearalenone and Its Major Modified Forms in Pigs. *Toxins (Basel), 9*(2), pii: E56.

Bridgham, J. T., Eick, G. N., Larroux, C., Deshpande, K., Harms, M. J., Gauthier, M. E. A., Ortlund, E. A., Degnan, B. M., & Thornton, J. W. (2010). Protein Evolution by Molecular Tinkering: Diversification of the Nuclear Receptor Superfamily from a Ligand-Dependent Ancestor. *Plos Biology, 8*(10).

Brzozowski, A. M., Pike, A. C., Dauter, Z., Hubbard, R. E., Bonn, T., Engström, O., Ohman, L., Greene, G. L., Gustafsson, J. A., & Carlquist, M. (1997). Molecular basis of agonism and antagonism in the oestrogen receptor. *Nature, 389*(6652), 753-758.

Carosati, E., Sciabola, S., & Cruciani, G. (2004). Hydrogen bonding interactions of covalently bonded fluorine atoms: from crystallographic data to a new angular function in the GRID force field. *Journal of Medicinal Chemistry, 47*(21), 5114-5125.

Cheron, J. B., Casciuc, I., Golebiowski, J., Antonczak, S., & Fiorucci, S. (2017). Sweetness

prediction of natural compounds. *Food Chemistry, 221*, 1421-1425.
Dalton, J. A. R., & Jackson, R. M. (2007). An evaluation of automated homology modelling methods at low target-template sequence similarity. *Bioinformatics, 23*(15), 1901-1908.
Dellafiora, L., Dall'Asta, C., & Cozzini, P. (2015). Ergot alkaloids: From witchcraft till in silico analysis. Multi-receptor analysis of ergotamine metabolites. *Toxicology Reports, 2*, 535-545.
Dellafiora, L., Dall'Asta, C., & Galaverna, G. (2018). Toxicodynamics of Mycotoxins in the Framework of Food Risk Assessment-An In Silico Perspective. *Toxins, 10*(2), E52.
Dellafiora, L., Dall'Asta, C., Cruciani, G., Galaverna, G., & Cozzini, P. (2015). Molecular Modelling approach to evaluate poisoning of topoisomerase I by alternariol derivatives. *Food Chemistry, 189*, 93-101.
Dellafiora, L., Galaverna, G., Cruciani, G., Dall'Asta, C., & Bruni, R. (2018). On the Mechanism of Action of Anti-Inflammatory Activity of Hypericin: An In Silico Study Pointing to the Relevance of Janus Kinases Inhibition. *Molecules, 23*(12), piiE3058.
Dellafiora, L., Galaverna, G., & Dall'Asta, C. (2017). In silico analysis sheds light on the structural basis underlying the ribotoxicity of trichothecenes - A tool for supporting the hazard identification process. *Toxicology Letters, 270*, 80-87.
Dellafiora, L., Galaverna, G., Dall'Asta, C., & Cozzini, P. (2015). Hazard identification of cis/trans-zearalenone through the looking-glass. *Food and Chemical Toxicology, 86*, 65-71.
Dellafiora, L., Warth, B., Schmidt, V., Del Favero, G., Mikula, H., Fröhlich, J., & Marko, D. (2018). An integrated in silico/in vitro approach to assess the xenoestrogenic potential of Alternaria mycotoxins and metabolites. *Food Chemistry, 248*, 253-261.
Devreese, M., Antonissen, G., Broekaert, N., De Baere, S., Vanhaecke, L., De Backer, P., & Croubels, S. (2015). Comparative Toxicokinetics, Absolute Oral Bioavailability, and Biotransformation of Zearalenone in Different Poultry Species. *Journal of Agricultural and Food Chemistry, 63*(20), 5092-5098.
Dong, G. L., Pan, Y. H., Wang, Y. L., Ahmed, S., Liu, Z. L., Peng, D. P., & Yuan, Z. H. (2018). Preparation of a broad-spectrum anti-zearalenone and its primary analogues antibody and its application in an indirect competitive enzyme-linked immunosorbent assay. *Food Chemistry, 247*, 8-15.
EFSA. (2011). Scientific Opinion on the risks for public health related to the presence of zearalenone in food. *EFSA J., 9, 2197*.
EFSA. (2017). Risks for animal health related to the presence of zearalenone and its modified forms in feed. *EFSA J., 15*(7), 4851.
Ehrlich, V. A., Dellafiora, L., Mollergues, J., Dall'Asta, C., Serrant, P., Marin-Kuan, M., Lo Piparo, E., Schilter, B., & Cozzini, P. (2015). Hazard assessment through hybrid in vitro/in silico approach: The case of zearalenone. *ALTEX, 32*(4), 275-286.
Escriva, H., Delaunay, F., & Laudet, V. (2000). Ligand binding and nuclear receptor evolution. *Bioessays, 22*(8), 717-727.
Gonçalves, R., Schatzmayr, D., Albalat, A., & Mackenzie, S. (2018). Mycotoxins in aquaculture: feed and food. *Reviews in Aquaculture, 0*(0), 1-31.
Gromadzka, K., Waskiewicz, A., Chelkowski, J., & Golinski, P. (2008). Zearalenone and its metabolites: occurrence, detection, toxicity and guidelines. *World Mycotoxins Journal, 1*(2), 209-220.
Gruber-Dorninger, C., Novak, B., Nagl, V., & Berthiller, F. (2017). Emerging Mycotoxins: Beyond Traditionally Determined Food Contaminants. *Journal of Agricultural and Food Chemistry, 65*(33), 7052-7070.

Ivanova, L., Karelson, M., & Dobchev, D. A. (2018). Identification of Natural Compounds against Neurodegenerative Diseases Using In Silico Techniques. *Molecules, 25*(8), E1847.

Le Guevel, R., & Pakdel, F. (2001). Assessment of oestrogenic potency of chemicals used as growth promoter by in-vitro methods. *Human Reproduction, 16*(5), 1030-1036.

Lehmann, L., Wagner, J., & Metzler, M. (2006). Estrogenic and clastogenic potential of the mycotoxin alternariol in cultured mammalian cells. *Food and Chemical Toxicology, 44*(3), 398-408.

Lewis, A., Kazantzis, N., Fishtik, I., & Wilcox, J. (2007). Integrating process safety with molecular modeling-based risk assessment of chemicals within the REACH regulatory framework: Benefits and future challenges. *Journal of Hazardous Materials, 142*(3), 592-602.

Lin, K., Zhang, L. W., Han, X., Xin, L., Meng, Z. X., Gong, P. M., & Cheng, D. Y. (2018). Yak milk casein as potential precursor of angiotensin I-converting enzyme inhibitory peptides based on in silico proteolysis. *Food Chemistry, 254*, 340-347.

Lohning, A. E., Levonis, S. M., Williams-Noonan, B., & Schweiker, S. S. (2017). A Practical Guide to Molecular Docking and Homology Modelling for Medicinal Chemists. *Current Topics in Medicinal Chemistry, 17*(18), 2023-2040.

Maldonado-Rojas, W., & Olivero-Verbel, J. (2011). Potential interaction of natural dietary bioactive compounds with COX-2. *Journal of Molecular Graphics & Modelling, 30*, 157-166.

Mally, A., Solfrizzo, M., & Degen, G. H. (2016). Biomonitoring of the mycotoxin Zearalenone: current state-of-the art and application to human exposure assessment. *Archives of Toxicology, 90*(6), 1281-1292.

Marin, S., Ramos, A. J., Cano-Sancho, G., & Sanchis, V. (2013). Mycotoxins: Occurrence, toxicology, and exposure assessment. *Food and Chemical Toxicology, 60*, 218-237.

Matthews, J., Celius, T., Halgren, R., & Zacharewski, T. (2000). Differential estrogen receptor binding of estrogenic substances: a species comparison. *The Journal of Steroid Biochemistry and Molecular Biology, 74*(4), 223-234.

Monzon, A. M., Zea, D. J., Marino-Buslje, C., & Parisi, G. (2017). Homology modeling in a dynamical world. *Protein Science, 26*(11), 2195-2206.

Nikolaev, D. M., Shtyrov, A. A., Panov, M. S., Jamal, A., Chakchir, O. B., Kochemirovsky, V. A., Olivucci, M., & Ryazantsev, M. N. (2018). A Comparative Study of Modern Homology Modeling Algorithms for Rhodopsin Structure Prediction. *Acs Omega, 3*(7), 7555-7566.

Nwachukwu, J. C., Srinivasan, S., Bruno, N. E., Nowak, J., Wright, N. J., Minutolo, F., Rangarajan, E. S., Izard, T., Yao, X. Q., Grant, B. J., Kojetin, D. J., Elemento, O., Katzenellenbogen, J. A., & Nettles, K. W. (2017). Systems Structural Biology Analysis of Ligand Effects on ER alpha Predicts Cellular Response to Environmental Estrogens and Anti-hormone Therapies. *Cell Chemical Biology, 24*(1), 35-45.

Pettersen, E. F., Goddard, T. D., Huang, C. C., Couch, G. S., Greenblatt, D. M., Meng, E. C., & Ferrin, T. E. (2004). UCSF Chimera--a visualization system for exploratory research and analysis. *Journal of Computational Chemistry, 25*(13), 1605-1612.

Phillips, C., Roberts, L., Schade, M., Bazin, R., Bent, A., Davies, N., Moore, R., Pannifer, A., Pickford, A., Prior, S., Read, C., Scott, A., Brown, D., Xu, B., & Irving, S. (2011). Design and structure of stapled peptides binding to estrogen receptors. *Journal of the American Chemical Society, 133*(25).

Pike, A. C. W., Brzozowski, A. M., & Hubbard, R. E. (2000). A structural biologist's view of the oestrogen receptor. *Journal of Steroid Biochemistry and Molecular Biology, 74*(5), 261-268.

Pitt, J. I. (2013). Mycotoxins. In G. J. Morris & E. M. Potter (Eds.), *Foodborne Infections and*

Intoxications 4th ed., (pp. 409-418): Academic Press.
Rollinger, J. M., Schuster, D., Baier, E., Ellmerer, E. P., Langer, T., & Stuppner, H. (2006). Taspine: bioactivity-guided isolation and molecular ligand-target insight of a potent acetylcholinesterase inhibitor from Magnolia x soulangiana. *Journal of Natural Products, 69*(9), 1341-1346.
Sali, A., & Blundell, T. L. (1993). Comparative protein modelling by satisfaction of spatial restraints. *Journal of Molecular Biology, 234*(3), 779-815.
Sonneveld, E., Riteco, J. A., Jansen, H. J., Pieterse, B., Brouwer, A., Schoonen, W. G., & van der Burg, B. (2006). Comparison of in vitro and in vivo screening models for androgenic and estrogenic activities. *Toxicological Sciences, 89*(1), 173-187.
Sonoda, M. T., Martinez, L., Webb, P., Skaf, M. S., & Polikarpov, I. (2008). Ligand dissociation from estrogen receptor is mediated by receptor dimerization: Evidence from molecular dynamics simulations. *Molecular Endocrinology, 22*(7), 1565-1578.
Spyrakis, F., & Cozzini, P. (2009). How computational methods try to disclose the estrogen receptor secrecy--modeling the flexibility. *Current Medicinal Chemistry, 16*(23), 2987-3027.
Tolosa, J., Font, G., Manes, J., & Ferrer, E. (2014). Natural Occurrence of Emerging Fusarium Mycotoxins in Feed and Fish from Aquaculture. *Journal of Agricultural and Food Chemistry, 62*(51), 12462-12470.
Zinedine, A., Soriano, J. M., Moltó, J. C., & Mañes, J. (2007). Review on the toxicity, occurrence, metabolism, detoxification, regulations and intake of zearalenone: an oestrogenic mycotoxin. *Food and Chemical Toxicology, 45*(1), 1-18.

Table 1. Docking results on human and rainbow trout ER

	H. sapiens		***O. mykiss***	
Compound	**Relative estrogenic activity (%)**	**Relative computed score**	**Relative estrogenic activity (%)**	**Relative computed score**
E2	100 [a]	1.000	100 [a]	1.000
αZEL	2.47 [a]	0.945 ± 0.001	43.33 [a]	0.851 ± 0.001
ZEN	0.57 [a]	0.912 ± 0.010	8.39 [a]	0.828 ± 0.001
βZEL	0.26 [a]	0.711 ± 0.008	< 0.01 [a]	0.451 ± 0.004
β-sitosterol	Inactive [b]	-2.028 ± 0.303	Inactive [b]	-1.696 ± 0.312
AOH	0.01[c]	0.814 ± 0.002	Not tested yet	0.709 ± 0.005

[a] (Le Guevel and Pakdel 2001)
[b] (Matthews et al. 2000)
[c] (Lehmann et al. 2006)

Figure 1. Chemical structures of molecules accounted in the study.

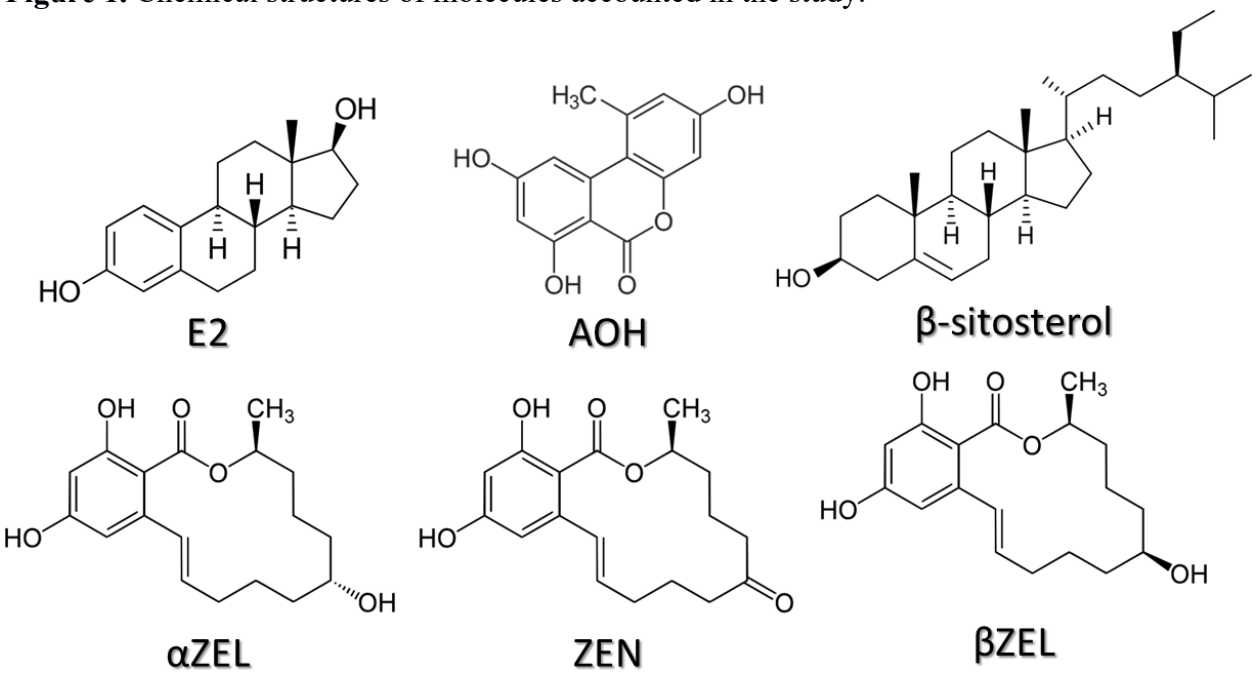

Figure 2. Sequence and structure alignments of human and trout ER. **A.** Sequence alignment of human and trout ER. Dots indicate conserved amino acids. The residues forming the binding site are highlighted in yellow, while L349/362M and M528/541I are indicated with red boxes. **B.** Superimposition of the 3D structures of human (white) (PDB ID 2YJA) (Phillips et al. 2011) and trout (yellow) ER represented in cartoon. The binding site is represented in mesh. **C.** Superimposition of binding sites of human (white) (PDB ID 2YJA) (Phillips et al. 2011) and trout (yellow) ER.

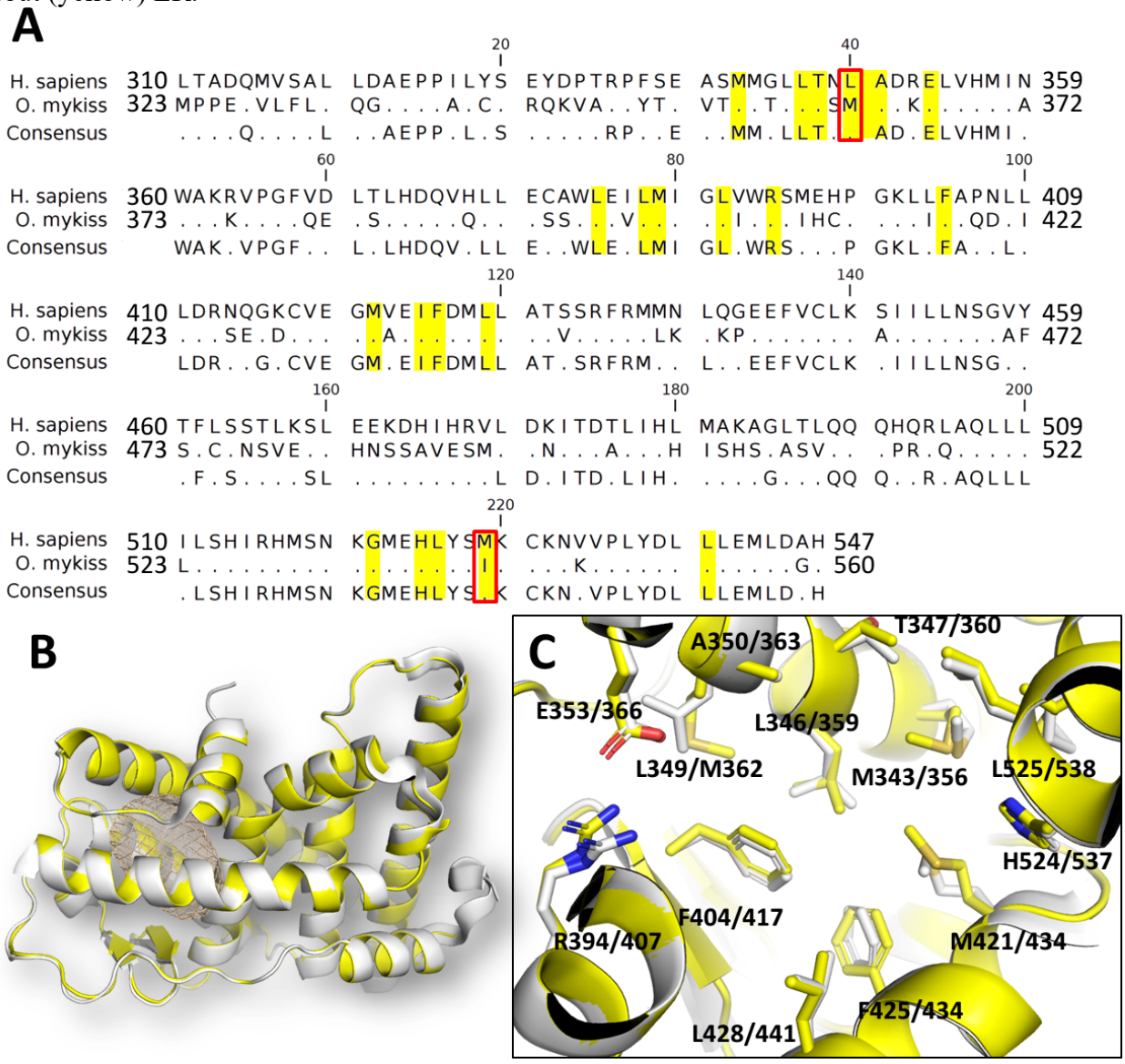

Figure 3 Figure 3. Comparison between the pockets of human and trout ER. **A.** Comparison between the shape of human (white) (PDB ID 2YJA) (Phillips et al. 2011) and trout (yellow) ER. The shape of the pockets is retraced in cut surface. The reshaping due to the M528/541I mutation is highlighted by the red arrow. **B.** Pharmacophoric differences between human and trout ER. The human pocket is reported and grey mesh indicates the differences of hydrophobic regions found in the two orthologous (i.e. the hydrophobic region found in the human pocket and not in the trout one).

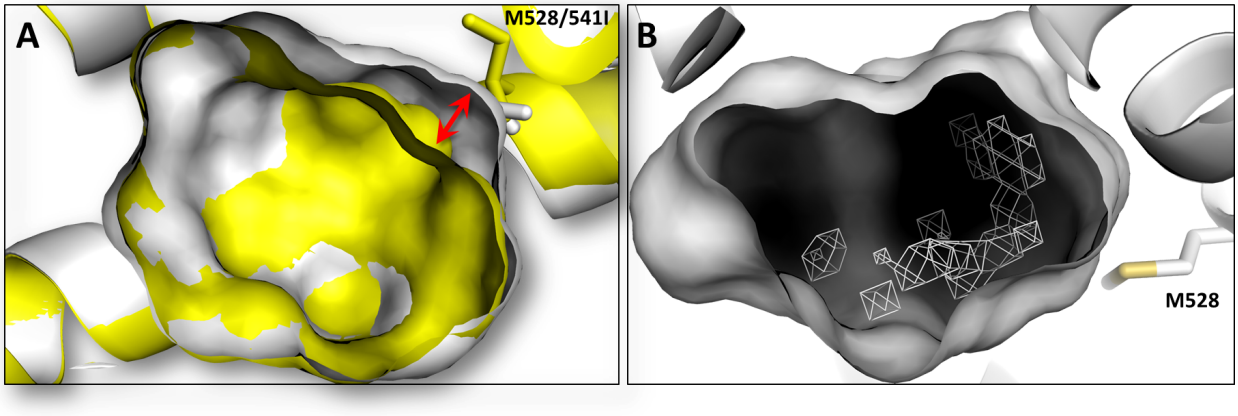

Figure 4. Binding architectures of ligands. Ligands are represented in sticks while ER is represented in cartoon. Unless otherwise specified, the crystallographic poses are reported in white, while in yellow and cyan are reported the computed poses within the human and trout ER, respectively. **A.** Computed pose of E2 in comparison with the binding architecture reported by crystallographic studies (PDB ID 2YJA) (Phillips et al. 2011). **B.** Computed pose of ZEN in comparison with the binding architecture reported by crystallographic studies (PDB ID 5KRC) (Nwachukwu et al. 2017). **C.** Computed pose of αZEL in comparison with the binding architecture reported by crystallographic studies (PDB ID 4TUZ) (Delfosse et al. 2014). **D.** Superimposition of crystallographic poses of αZEL (pale yellow) and E2 (white). **E.** Comparison between the crystallographic pose of E2 (PDB ID 2YJA) (Phillips et al. 2011), with the computed poses of βZEL within the human and trout ER. The black arrow indicates the different orientation the ligand calculated within the trout ER in comparison to the one showed into the human pocket. **F.** Comparison between the crystallographic pose of E2, with the computed poses of AOH within the human and trout ER.

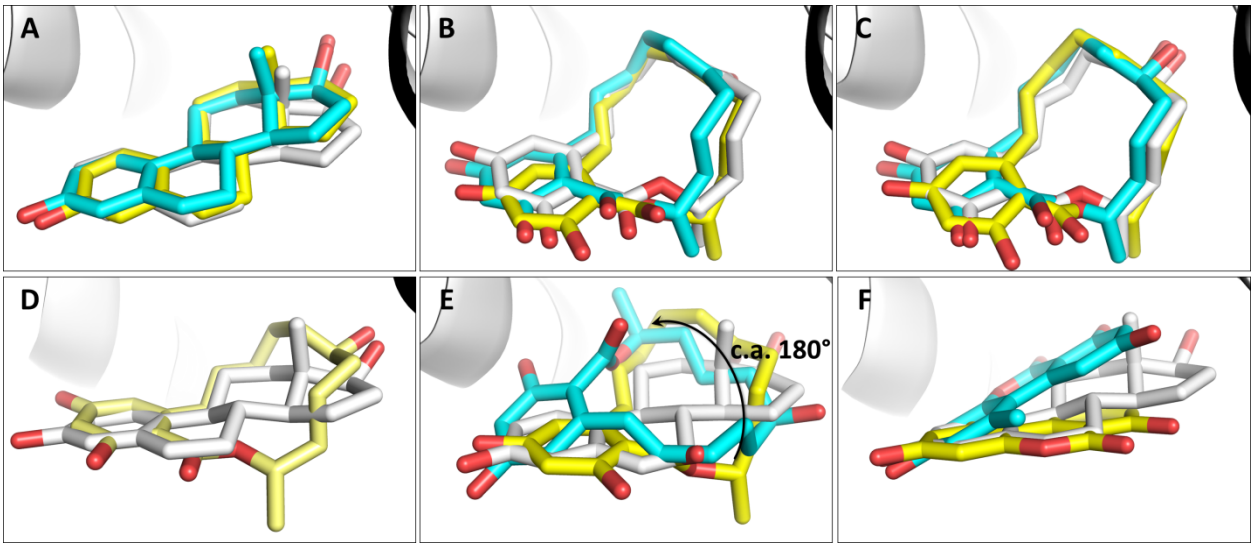

Figure 5. Conformational changes of human ER complexes. **A.** RMSD plot of human ER C-α in complex with E2, ZEN, βZEL or AOH. **B.** RMSD plot of E2, ZEN, βZEL or AOH. **C.** Hydrogen bonds blot of human ER in complex with E2, ZEN, βZEL or AOH.

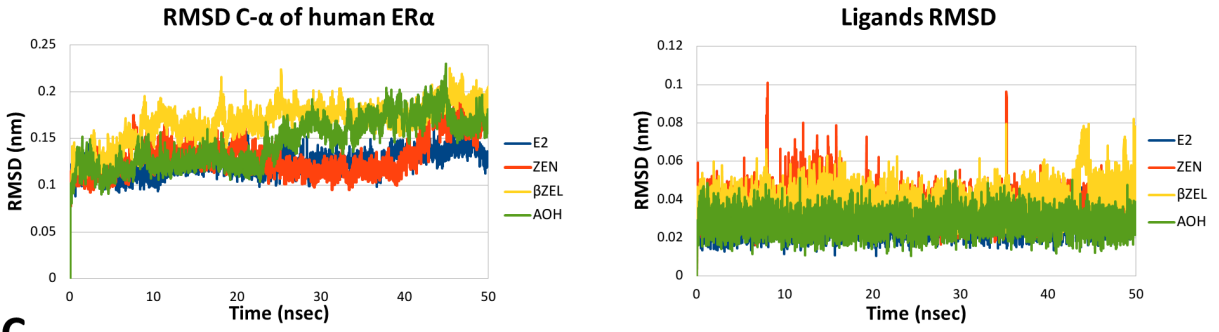

C

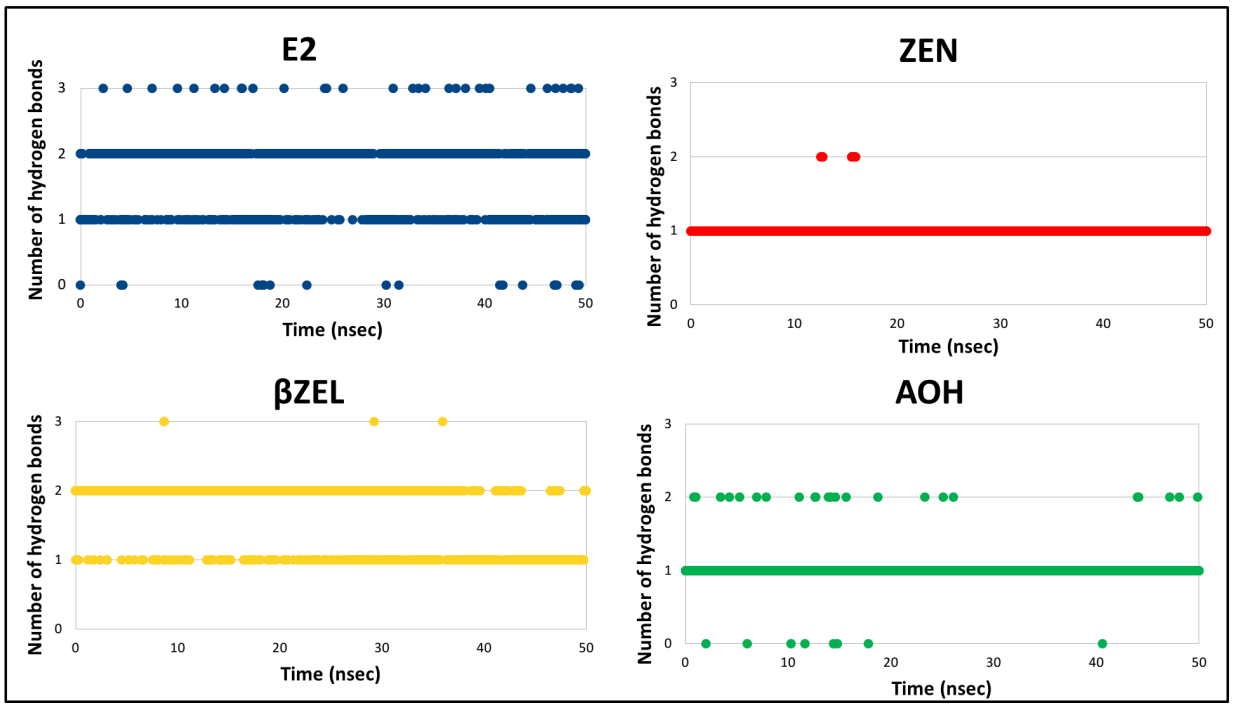

Figure 6. Conformational changes of trout ER complexes. **A.** RMSD plot of trout ER C-α in complex with E2, ZEN, βZEL or AOH. **B.** RMSD plot of E2, ZEN, βZEL or AOH. **C.** Hydrogen bonds blot of trout ER in complex with E2, ZEN, βZEL or AOH. **D.** Crystallographic pose of ZEN (white) (PDB ID 5KRC) (Nwachukwu et al. 2017) in comparison to the two discrete different poses of βZEL calculated along the simulation (in green is shown the starting pose, while in blue is shown the pose adopted during the simulation). The black arrow indicates the re-orienteering of the molecule during the simulation in respect to the optimal orientation of ZEN. **E.** RMSF plot of residues C-α of trout ER in complex with E2, ZEN, βZEL or AOH. Black boxes indicate the region found differentially flexible and related to protein activity. The localization of such regions on the ER structure is highlighted in red in the protein representation reported above the plot.